RNA (1999), *5*:1149–1157. Cambridge University Press. Printed in the USA.

A stable hairpin preceded by a short open reading frame promotes nonlinear ribosome migration on a synthetic mRNA leader

MAJA HEMMINGS-MIESZCZAK and THOMAS HOHN
Friedrich Miescher-Institut, CH-4058 Basel, Switzerland

ABSTRACT

The regulation of cauliflower mosaic virus (CaMV) pregenomic 35S RNA translation occurs via nonlinear ribosome migration (ribosome shunt) and is mediated by an elongated hairpin structure in the leader. The replacement of the viral leader by a series of short, low-energy stems in either orientation supports efficient ribosomal shunting, showing that the stem *per se*, and not its sequence, is recognized by the translation machinery. The requirement for *cis*-acting sequences from the unstructured terminal regions of the viral leader was analyzed: the 5′-terminal polypyrimidine stretch and the short upstream open reading frame (uORF) A stimulate translation, whereas the 3′-flanking region seems not to be essential. Based on these results, an artificial leader was designed with a stable stem flanked by unstructured sequences derived from parts of the 5′- and 3′-proximal regions of the CaMV 35S RNA leader. This artificial leader is shunt-competent in translation assays in vivo and in vitro, indicating that a low-energy stem, broadly used as a device to successfully interfere with ribosome scanning, can efficiently support translation, if preceded by a short uORF. The synthetic 140-nt leader can functionally replace the CaMV 35S RNA 600-nt leader, thus implicating the universal role that nonlinear ribosome scanning could play in translation initiation in eukaryotes.

Keywords: pararetrovirus; RNA structure; translation initiation

INTRODUCTION

In eukaryotic cells, translation initiation usually occurs according to the ribosome scanning mechanism (Kozak, 1989b). This classical model assumes that, at first, the 40S preinitiation complex associates with an mRNA at the 5′-terminal cap structure and later unidirectionally scans the mRNA leader until the first AUG codon positioned in an appropriate context is encountered, whereupon the 60S subunit joins and protein synthesis starts. Translation can be strongly affected by *cis*-acting elements and *trans*-acting factors that interfere with ribosome scanning in the leader: (1) highly stable stem-loop structures mechanically block scanning by stalling 40S subunits on the 5′ site of the hairpin (Pelletier & Sonenberg, 1985; Kozak, 1986, 1989a); (2) upstream open reading frames (uORFs) reduce initiation downstream due to the apparent low efficiency of reinitiation at subsequent AUG codons (Kozak, 1989b, 1992; Hinnenbusch, 1994); (3) RNA-binding proteins associated with cap-proximal binding sites inhibit recognition of the cap structure due to the steric hindrance (Gray & Hentze, 1994; Stripecke et al., 1994). Modified ribosome scanning mechanisms exist, however, that allow relatively efficient translation despite the presence of inhibitory elements in the leader. Alternative modes of translation initiation have been broadly studied and fall into several categories: leaky scanning (Kozak, 1992), reinitiation (Geballe & Morris, 1994; Hinnenbusch, 1994), internal initiation (Pelletier & Sonenberg, 1988; Kaminski et al., 1990; Belsham, 1992), and nonlinear ribosome scanning or ribosome shunt (Curran & Kolakofsky, 1988, 1989; Fütterer et al., 1989, 1993, 1996; Yueh & Schneider, 1996).

The cauliflower mosaic virus (CaMV) pregenomic 35S RNA 600-nt leader (Figs. 1 and 2A) contains all three elements with the potential to strongly inhibit translation: (1) a low-energy elongated hairpin (−110 kcal/mol) that has been characterized by enzymatic and chemical probing (Hemmings-Mieszczak et al., 1997), (2) several uORFs, and (3) a purine-rich cloverleaf structure that interacts with the CaMV coat protein (O. Guerra-Peraza, M. de Tapia, T. Hohn, and M. Hemmings-Mieszczak, submitted). However, translation initiation

Reprint requests to: Maja Hemmings-Mieszczak, Friedrich Miescher-Institut, Maulbeerstrasse 66, CH-4058 Basel, Switzerland; e-mail: mieszcza@fmi.ch.

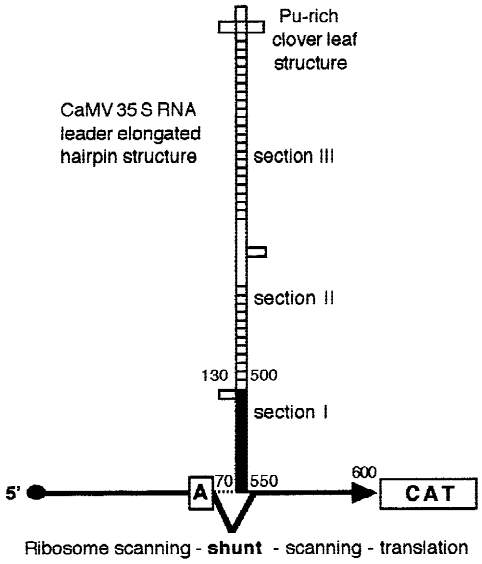

FIGURE 1. Nonlinear ribosome migration during translation initiation on the CaMV 35S RNA leader. The 600-nt leader is represented schematically as a combination of unstructured 5′- (nt 1–70) and 3′-proximal (nt 550–600) regions flanking an elongated hairpin structure (nt 70–550). The three stem sections of different stability are labeled I, II, and III. The stable interaction within stem section I promotes translation of a downstream CAT reporter gene by the ribosome shunt mechanism. Essential elements: 5′ cap, uORF A, and stable stem section I are indicated. The 5′-to-3′ unidirectional ribosome migration is described below the figure.

downstream of the leader is cap dependent and relatively efficient. The hairpin structure with the uORFs does not inhibit translation, as might be expected, but is excluded from the scanning process because of nonlinear ribosome migration (Fütterer et al., 1989, 1993). The biological role of the elongated hairpin structure in the CaMV 35S RNA leader has recently been analyzed: translation analysis performed in vivo and in vitro has demonstrated that formation of the stable hairpin in the leader is absolutely required for optimal shunting (Hemmings-Mieszczak et al., 1998). A mutational screen demonstrated the importance of the short uORF A terminating 6 nt upstream of the hairpin structure. Cauliflower mosaic viruses bearing a mutation of the uORF A initiation codon have reduced infectivity and always revert at first or second sites (Pooggin et al., 1998); a deletion of uORF A was shown to affect translation in vitro (Dominguez et al., 1998). In summary, a combination of *cis*-acting elements seems to be both essential and sufficient to stimulate nonlinear ribosome scanning on the CaMV 35S RNA leader.

The current model of the ribosome shunt predicts that, after the initial cap-dependent scanning, the ribosome translates uORF A, bypasses the stable hairpin structure, and resumes scanning downstream (Fig. 1). The details of the ribosome shunt mechanism remain unclear and difficult to study on the multifunctional viral leader. Therefore, we have designed an artificial mRNA leader of 140 nt that can mimic and replace the CaMV 35S RNA 600-nt leader originally used in the ribosome shunt studies. The CAT reporter gene under the control of the synthetic leader was assayed for translation in vivo in transiently transfected protoplasts and in vitro in wheat germ extract. The functional mimicry by the synthetic model molecule reveals the universal role that nonlinear ribosome migration might play in translation initiation in eukaryotes.

RESULTS

5′- but not 3′-proximal sequences in the CaMV 35S RNA leader affect translation

The impact of the *cis*-acting elements from both unstructured regions of the CaMV 35S RNA leader (Fig. 1) was monitored by translation of the CAT-reporter gene placed downstream of mutated versions of the leader. For these experiments, we used a CaMV 35S RNA leader-cassette expression construct, in which additional restriction sites allow easy introduction of mutations and structural replacements within the leader region (Fig. 2A). Generally, results were similar whether the constructs were analyzed in vivo in transiently transfected plant protoplasts or in vitro in wheat germ extract (summarized in Table 1).

All mutations within the 5′-proximal region (Fig. 2B) have a strong impact on translation (Fig. 3A). Deletion of two pyrimidine repeats results in moderate repression (by a factor of 2 to 3; pMH176), indicating that they might function as weak translational enhancers. Deletion of uORF A substantially decreases translation (up to 85% inhibition; pMH174), as could be expected from a previous study on mutated virus *in planta* (Pooggin et al., 1998) and translation analysis performed in vitro, albeit on another CaMV strain (Dominguez et al., 1998). An almost complete deletion of the 5′-proximal unstructured domain (pMH119) fully abolishes translation. These results suggest that: (1) translation or recognition of the uORF A is required for the downstream ORF expression, rather than for structural rearrangements leading to internal ribosome entry site (IRES) formation, as could be hypothesized; (2) the extended stem-loop structure might be sufficiently stable to block scanning ribosomes.

The 3′-proximal 50-nt region (Fig. 2C) contains two purine-rich tracks interrupted by a cytosine-rich element, the latter being involved in formation of a long-range pseudoknot (ψ_B; Hemmings-Mieszczak et al., 1997). Deletions or substitutions of these sequences (pMH150 to pMH169) do not affect translation (Fig. 3A), neither does deletion of the formyl-Met tRNA primer binding site for reverse transcription (pMH177). Other sequences from the 3′-proximal region also seem not to be essential, as translation initiation is unaffected even by large deletions in this region (pMH187).

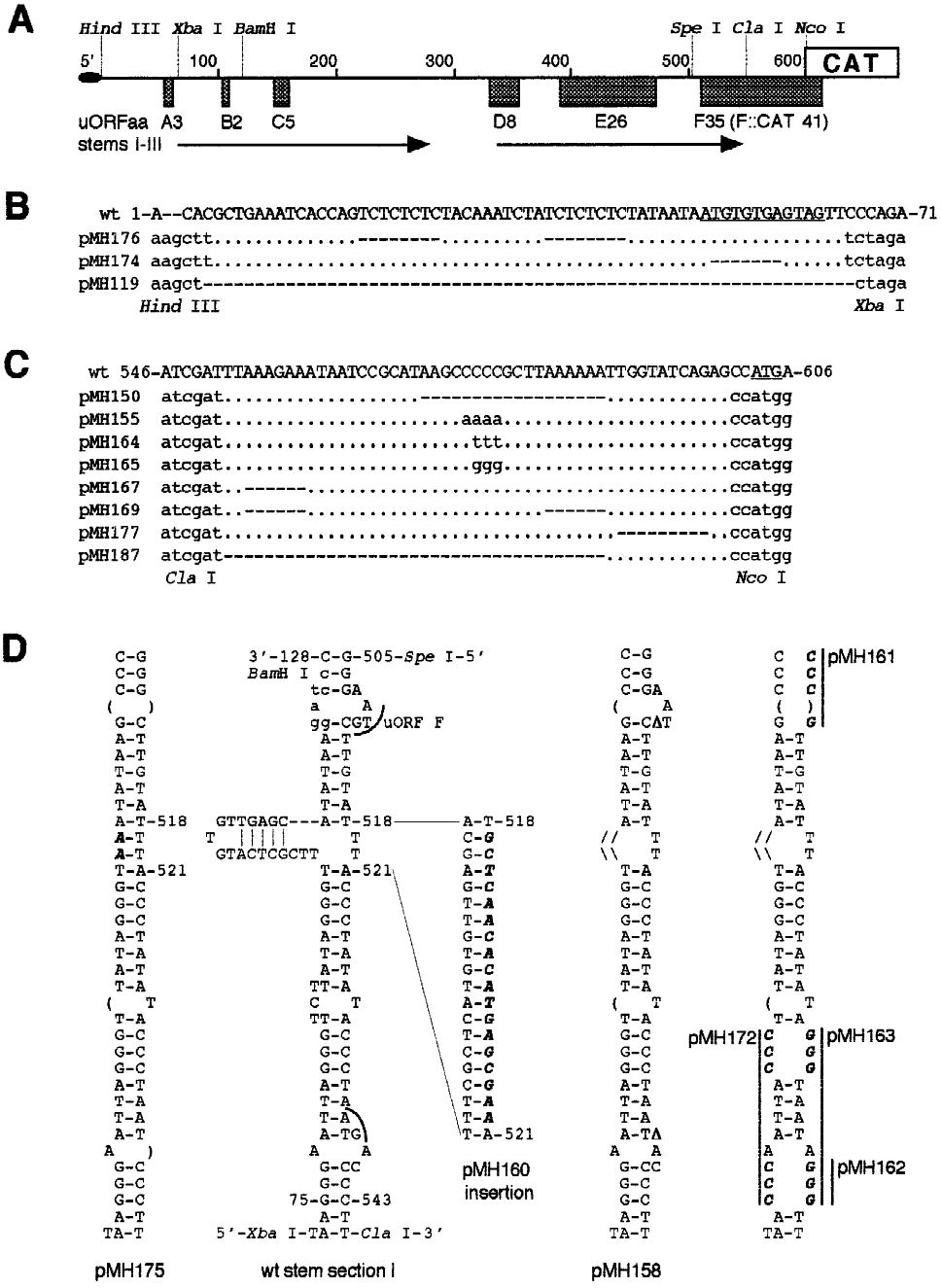

FIGURE 2. CaMV 35S RNA leader constructs. **A**: Schematic representation of the leader-cassette shown to scale, with numbering every 100 nt. The 5′-cap modification is indicated by a black oval; the uORFs are named by letters and depicted as boxes with numbers denoting their coding capacities. Horizontal arrows correspond to the base paired regions forming the elongated hairpin structure (nt 70–550). Natural (*Cla*I) and additionally introduced restriction sites (*Hin*dIII, *Xba*I, *Bam*HI, *Eco*RI, *Spe*I, and *Nco*I) are indicated. Construction of restriction sites and CAT-reporter gene fusions are described in Materials and Methods. **B**,**C**: Primary sequence and mutations in the 5′- and the 3′-proximal unstructured regions, respectively. Wild-type sequence is represented by capital letters, restriction sites are depicted in lower case. Deletions (dashes), conserved nucleotides (dots) and substitutions (lower case) are indicated. uORF A, encoded within the 5′-proximal region, and the initiation codon of the downstream CAT-ORF in the 3′-proximal region are underlined. **D**: Secondary structure of the elongated hairpin stem section I with multiple point mutations shown in bold; deletions of G-nucleotides to remove initiation codons of uORF F in pMH158 are denoted by (Δ).

TABLE 1. Mutations introduced in the CaMV 35S RNA leader and their effects on expression of the CAT-reporter gene in vitro and in transiently transfected *O. violaceus* protoplasts.[a]

Construct	Mutation type and location	CAT translation		Comments on ribosome shunt
		in vivo	in vitro	
CaMV leader	additional restriction sites	100	100	as wild-type, no or little scanning
pMH176	5′: Δ(CU)	29	42	weak enhancer
pMH174	5′: Δ uORF A	13	16	essential > model leader
pMH119	5′: Δ 1–69	5	5	essential > model leader
pMH150	3′: $\Delta\psi_B$	95	101	no effect
pMH155	3′: $\Delta\psi_B$ (C > A)	88	115	no effect
pMH164	3′: $\Delta\psi_B$ (C > T)	83	90	no effect
pMH165	3′: $\Delta\psi_B$ (C > G)	77	69	no effect
pMH167	3′: Δ Pu-1	132	100	no effect
pMH169	3′: Δ Pu-1, -2	106	98	no effect
pMH177	3′: ΔPBS	75	84	no effect
pMH187	3′: Δ 552–588	95	94	no effect
pMH175	st I: Δ uORF B	103	98	no effect
pMH158	st I: Δ AUG of uORF F	118	90	no effect
pMH160	st I: stronger structure	81	103	no effect
pMH161	st I: weak structure	25	50	scanning to uORF F
pMH162	st I: weak structure	4	6	scanning to uORF F
pMH163	st I: weak structure	12	4	scanning to uORF F
pMH172	st I: weak structure	12	4	inhibition
pMH215	st I: 158 & 163	n.a.	3	negative control
pMH188	st I: stem replacement	106/100	170/100	essential = model leader
pMH189	st I: antisense 188 stem	117	95	no effect
pMH190	st I: extended 188 stem	131	105	no effect
pMH191	5′: 188 & Δ uORF A	3	20	essential > model leader
pMH212	5′: 188 & Δ 1–69	2	6	essential > model leader
pMH200	3′: 188 & Δ 552–588	78	74	no effect = short model leader
Controls:				
pMH192	190 stem & uAUG-near	81	101	no effect
pMH193	190 stem & uAUG-far	88	93	no effect
pMH195	188 stem & uAUG	76	96	no effect
pMH197	192 & Δ 552–588 (10aa::CAT)	104	86	no effect
pMH198	193 & Δ 552–588 (16aa::CAT)	78	83	no effect
pMH199	195 & Δ 552–588 (14aa::CAT)	88	74	no effect
pMH206	linear R-198 (16aa::CAT)		+	positive control
pMH208	linear R-199 (14aa::CAT)		+	positive control
pMH210	linear R-197 (10aa::CAT)		+	positive control

[a] Translation efficiencies represent average values from three independent experiments. n.a.: not analyzed.

The elongated hairpin in the CaMV 35S RNA leader blocks ribosome scanning, but stimulates shunting

Regulation of CaMV 35S RNA translation is mediated by the stable hairpin in the leader (Hemmings-Mieszczak et al., 1998). As was shown previously, a structural mutation that additionally stabilizes its structure has no effect on downstream reporter gene expression (pMH160; Figs. 2D and 3B). The elongated hairpin of the 35S RNA leader includes five uORFs: uORF B to F. Mutations of two of those uORFs, that is, deletion of uORF B (pMH175) or mutation of both AUG codons from uORF F (pMH158), do not influence CAT expression (Figs. 2D and 3B). In contrast, structural mutations that destabilize the elongated hairpin in the leader were shown to decrease expression of the downstream CAT-reporter gene, both in vivo and in vitro (Hemmings-Mieszczak et al., 1998; Figs. 2D and 3B; pMH161, pMH162, pMH163, and pMH172). We assume that upon diminished ribosome shunting, more efficient scanning through the middle part of the leader should occur, resulting in higher expression of uORFs B to F. Thus, translation of the longest one, uORF F, which in our constructs overlaps out-of-frame with the CAT ORF, could be used to monitor the level of ribosome scanning.

In vitro translation products were analyzed in an electrophoretic system (Schägger & von Jagow, 1987) that allows separation of the 4.6- and 7.9-kDa peptides derived from uORF F and the truncated CAT reporter gene, respectively (Fig. 4A). An additional weak band migrating at the position of the expected uORF F product was indeed detected in the case of mutants with decreased stability within stem section I (pMH161,

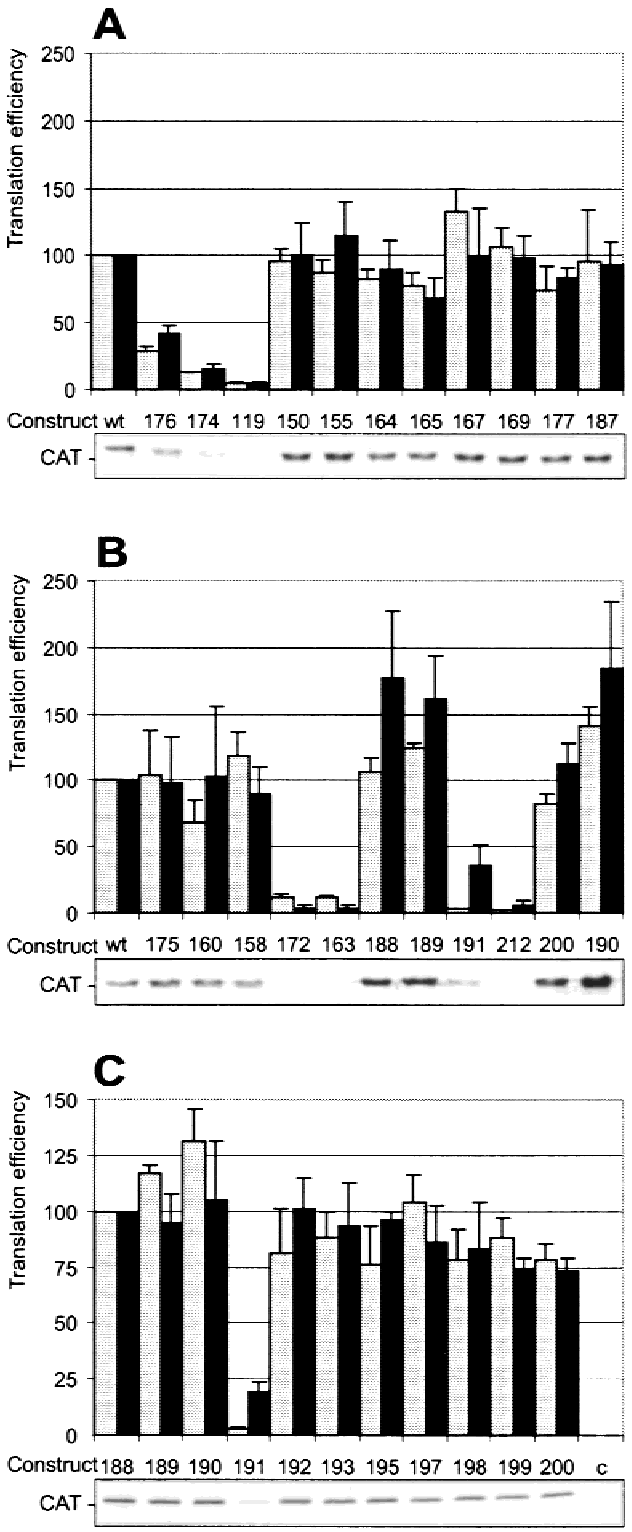

FIGURE 3. Expression of the CAT-reporter gene under control of mutations in the leader. **A**: Mutations in the 5′ end (pMH176, pMH174, pMH119), 3′ end (pMH150, pMH155, pMH164, pMH165, pMH167 pMH169, pMH177, pMH187). **B,C**: Structural mutations in stem section I (pMH175, pMH160, pMH158, pMH72, pMH163) and an artificial hairpin replacement in the CaMV 35S RNA leader (pMH188, pMH189, pMH191, pMH212, pMH200, pMH190). Mutations as depicted in Figures 2 and 5; expression levels in vivo and in vitro are represented by grey and black bars, respectively; resolution of in vitro translated products in 12% SDS-PAGE is shown in the lower panels; c in **C** indicates control with no external RNA included.

pMH162, pMH163, and pMH172; Fig. 4A, lanes 3–6). Lower salt concentration (50 mM potassium acetate) in the translation mixture can further destabilize the leader structure, resulting in decreased shunting (monitored by diminished expression of CAT; Fig. 4A, compare lanes 2 and 8) and enhanced scanning through the leader (monitored by increased expression of the uORF F; Fig. 4A, compare lanes 3 to 7 and 9 to 12). Identification of the expected ORF F product was indirectly confirmed with the help of mutant pMH215, where, in the context of structural mutation pMH163, both AUG codons from uORF F were removed and the band representing the corresponding peptide was missing (Fig. 4A, lanes 7 and 13). For immunodetection, the uORF F was C-terminally tagged with the HA-epitope (see Materials and Methods), precisely replacing the C-terminal uORF F extension into the CAT ORF (Fig. 4A, constructs wt′, 161′, 162′, 172′, 163′, and 215′). Translation in low salt conditions resulted in relatively high expression of the expected labeled uORF F::HA peptide (Fig. 4A, lanes 14–19) that can be specifically immunoprecipitated using the anti-HA antibody (Fig. 4B, lane 18). In this experiment, we could not detect any expression of uORF F in the wt leader constructs (Fig. 4A, lanes 2, 8, and 14), meaning that the wild-type elongated hairpin is indeed stable enough to prevent scanning through the middle part of the leader.

In summary, our results show that stability of the elongated hairpin plays a crucial role in blocking ribosome scanning and stimulating ribosome shunting on the CaMV 35S RNA leader. Thus, it seems interesting to test whether making a functional replacement is possible by introducing an unrelated structural element into the mRNA leader to promote ribosome shunting.

A stable artificial hairpin mimics the elongated hairpin function of the CaMV 35S RNA leader by blocking ribosome scanning and stimulating shunting

Artificial hairpins (Fig. 5A) were designed and cloned between the *Xba*I and *Cla*I restriction sites of the CaMV 35S RNA leader-cassette (Fig. 2A) to replace the natural elongated hairpin structure of the wild-type leader. All secondary structures used were based on published data demonstrating that an artificial stable hairpin can efficiently block 40S subunit scanning, even if not in direct proximity to the 5′-terminal cap structure in the leader (Kozak, 1989a). Thus, hp7-type structures flanked by the CaMV 35S RNA leader terminal sequences were tested in translation in vivo and in vitro (Fig. 3B). In both systems, replacement of the CaMV elongated hairpin structure by a short, low-energy stem, in either orientation (pMH188: −45 kcal/mol; pMH189: −46 kcal/mol), supports efficient translation, showing that the stem *per se*, and not its sequence, is recognized by the translation machinery. Stability of the hair-

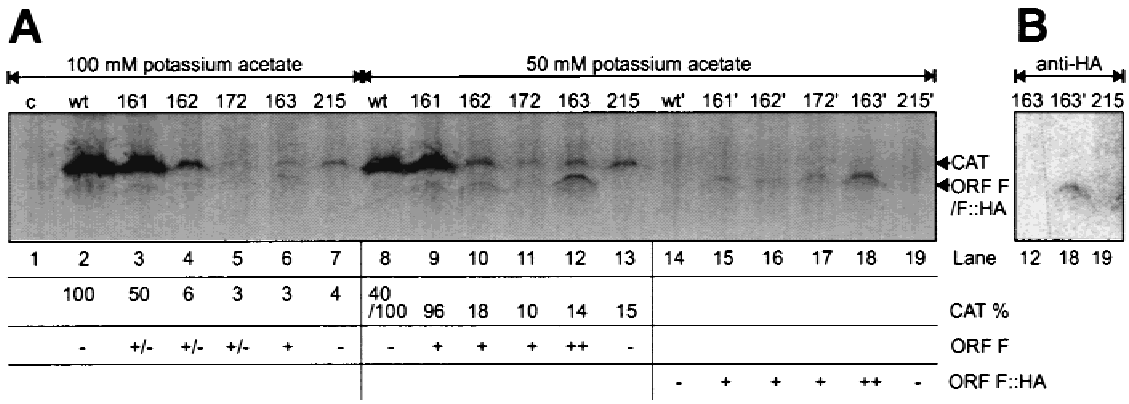

FIGURE 4. Expression of the CAT-reporter gene, uORF F, and uORF F::HA under control of structural mutations introduced in the CaMV 35S RNA leader. **A**: Resolution of in vitro-translated products in 16.5% SDS-PAGE using the Tricine discontinuous buffer system. Constructs as depicted in Figure 2 and Table 1; translation efficiency and migration of CAT, as well as migration of uORF F (wt, pMH161, pMH162, pMH163, pMH172, pMH215) or uORF F::HA (wt′, pMH161′, pMH162′, pMH163′, pMH172′, pMH215′) are indicated. **B**: Immunoprecipitation of the uORF::HA from pMH163, pMH163′, and pMH215′ translation in vitro.

pin in pMH188 seems to be sufficient to support ribosome shunting, as extending the structure does not enhance translation further (Fig. 3B; pMH190; −50 kcal/mol).

To analyze the mechanism of translation initiation on pMH188, we then introduced additional mutations that were previously found to affect translation under the control of the CaMV 35S RNA leader. Deletion of uORF A and deletion of the complete 5′-proximal unstructured region (Table 1; pMH191 and pMH212, respectively) seriously diminished translation when tested in the context of the pMH188 construct; deletion of most of the 3′-proximal unstructured region (pMH200) had only a marginal effect on CAT expression (equivalent to constructs pMH174, pMH119, and pMH187 in the CaMV 35S RNA leader context, respectively; see Figs. 2 and 5 for sequence of mutants). In vitro, as with constructs expressed under the control of the CaMV 35S RNA leader (Hemmings-Mieszczak et al., 1998), translation on the pMH188 transcript is optimal at 30 °C and a potassium acetate concentration of 100 mM (Fig. 6A). Altogether, the way the artificial low-energy stem supports translation in pMH188 appears similar to the translation mechanism occurring on the CaMV 35S RNA leader.

Generally, expression levels in vivo on the CaMV 35S RNA leader constructs parallel translation data in vitro indicating that our results reflect differences in translation efficiencies (Fig. 3A). Constructs including artificial hairpins were expressed at a similar level in vivo as those under the control of the CaMV 35S RNA leader (Fig. 3B); in in vitro experiments, however, their expression was slightly higher. Differences in ionic-strength conditions between the two translation systems might be responsible for this effect. In any case, when compared between themselves, all constructs with synthetic stems in the leader are expressed with similar efficiencies in vivo and in vitro (Fig. 3C). The level of CAT translation from these constructs is not influenced by additional upstream AUG (uAUG) codons introduced within the loops of the artificial secondary structure elements (pMH192, pMH193, and pMH195; Figs. 3C and 5A). This result suggests that, as with the CaMV 35S RNA leader constructs, ribosome scanning through the artificial secondary structures does not occur or is very inefficient. We introduced a deletion within the unstructured 3′-proximal region of the leader in pMH192, pMH193, and pMH195, allowing in-frame fusion of the additional uAUG codons to the CAT ORF (creating pMH197, pMH198, and pMH199, respectively; Fig. 5B). In fact, we could not detect the uAUG::CAT fusion product in any of the latter constructs, although these uAUG codons can act as initiation codons if positioned out of the hairpin context in the leader, as in pMH206, pMH208, and pMH210 (Figs. 5B and 6B). These results confirm that the artificial hairpins tested in our constructs fully inhibit ribosome scanning, but at the same time efficiently promote ribosome shunting, thus allowing translation of an ORF positioned downstream.

DISCUSSION

To date, translation initiation by nonlinear ribosome migration has been reported only for a few viral mRNAs. Viral multifunctional leaders, usually overloaded with RNA processing or packaging signals, could potentially interfere with the classical ribosome scanning. Shunting has been described in viruses infecting animal cells, such as Sendai virus (Curran & Kolakofsky, 1988, 1989), adenovirus (Yueh & Schneider, 1996) and budgerigar fledgling disease virus, BFDV (Li, 1996), as well as in plant-infecting pararetroviruses, CaMV (Fütterer et al., 1989, 1993), and rice tungro bacilliform virus, RTBV

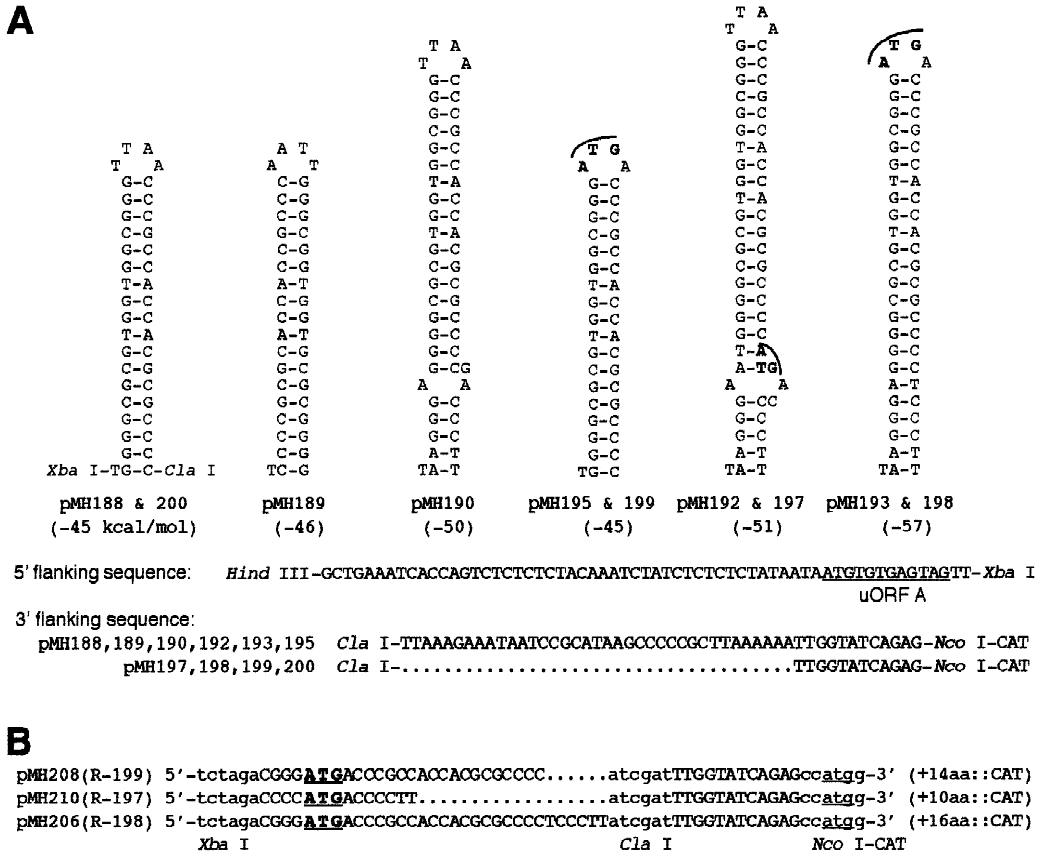

FIGURE 5. Artificial mRNA leader constructs. **A**: Secondary structures replacing an elongated hairpin in the CaMV 35S RNA leader. Restriction sites used for cloning, additional ATG initiation codons, and stem energies (kcal/mol) are indicated. **B**: Linear leaders pMH208, pMH210, and pMH206 with sequences corresponding to the right arms (R-) of stems from pMH199, pMH197, and pMH198, respectively. Restriction sites are written in lower case, additional ATG initiation codons are underlined. Sequences are aligned to show similarity with gaps depicted by dots. Expected extensions of the CAT-reporter gene products are shown in parentheses on the right.

(Fütterer et al., 1996). Expression of reporter genes under the influence of the shunt-competent CaMV and RTBV pregenomic RNA leaders has been studied in a broad range of experimental conditions: in transiently transfected plant protoplasts (Fütterer et al., 1993), in vitro (Schmidt-Puchta et al., 1997), and *in planta* (Schärer-Hernández & Hohn, 1998). Ribosome shunt occurs in plant tissues and cell cultures derived from both CaMV host and nonhost plants, indicating that shunting does not depend on host-specific factors. In this work, we demonstrate that ribosome shunt occurs on a synthetic mRNA leader just as well as on the viral leader. Although it has been documented only for a few mRNAs, nonlinear ribosome migration seems to operate in diverse systems and therefore might be considered as a general alternative mechanism for the initiation of translation in eukaryotes.

Nonlinear ribosome migration remains a rather poorly described mechanism for translation initiation in eukaryotes. Extensive studies on the CaMV pregenomic 35S RNA have shown that ribosome shunt depends exclusively on *cis*-acting elements in the leader: a low-energy, elongated hairpin structure preceded by a short ORF terminating upstream (Dominguez et al., 1998; Hemmings-Mieszczak et al., 1998; Pooggin et al., 1998). In some of the other cases where shunting has been reported, stable stems also seem to be involved (Fütterer et al., 1996; Li, 1996; Yueh & Schneider, 1996). Based on the common structural features of the known viral shunt-competent leaders, a synthetic mRNA leader was designed, where the viral structure is precisely replaced by a short, low-energy hairpin. This particular stem (Fig. 5A) has been previously used as a device to efficiently interfere with scanning: too stable to be unwound by the scanning complex, it does provoke the 40S subunit stalling on the 5′ side of the hairpin (hp7; Kozak, 1989a). Incorporation of the artificial hairpin within the viral flanking sequences indeed fully blocks ribosome scanning, but promotes efficient shunting (Table 1; pMH192, pMH193, and pMH195).

The best-studied artificial structured leader, pMH188, retains all the features of the original CaMV 35S RNA leader in our translation assays in vivo and in vitro. In both cases translation is cap dependent and stimulated

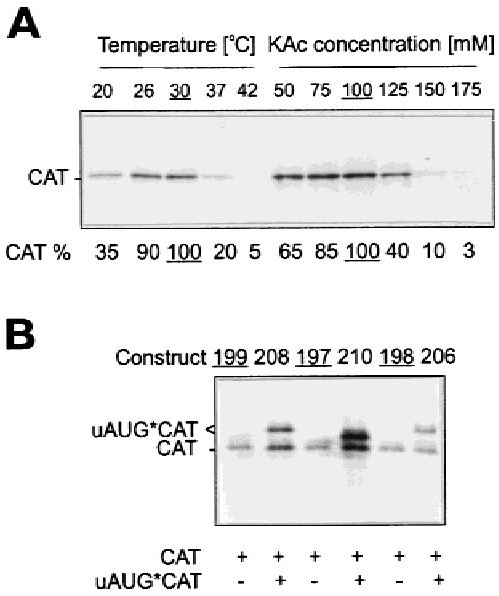

FIGURE 6. Expression of the CAT-reporter gene under control of the artificial leader. **A**: Optimum temperature and salt concentration of pMH188 translation in vitro analyzed in 12% SDS-PAGE. **B**: Resolution of in vitro-translated proteins in the 16.5% SDS-PAGE using the Tricine buffer system. Constructs and mutations are as depicted in Figure 5 and Table 1; constructs containing additional upstream ATT initiation codons in the hairpins are underlined; CAT and extended CAT-derived products are indicated.

by *cis*-acting elements in the 5′-proximal region (compare constructs pMH119, pMH176, and pMH212). The termination of uORF A in front of the stem structure seems to be of special importance: its deletion abolishes translation on both the viral and the synthetic leader (pMH174 and pMH191). In contrast, the role of the 3′-flanking sequence is negligible, as even large deletions in this region are well tolerated (pMH187 and pMH200). By analogy to the viral IRES structure and function (Pilipenko et al., 1992; Scheper et al., 1994), it was previously hypothesized that the 3′-proximal pyrimidine-rich sequences could form a "shunt acceptor site," that is, a landing pad for the shunting ribosomes (Fütterer et al., 1993; Dominguez et al., 1998). In this light, the latter result is rather surprising and suggests that the first AUG codon downstream of the stem might be a proper recognition signal for the ribosomes that have just accomplished shunting.

In the current study, we have constructed and tested several short, artificial mRNA leaders (summarized in Table 1) to replace the multifunctional 600-nt CaMV 35S RNA leader, previously used to study nonlinear migration. Our results indicate that the 140-nt leader from pMH200 or "the second best" 180-nt mRNA leader from pMH188 can be considered as the simplest shunt-competent model mRNA leaders. We have shown that a stable hairpin preceded by a short uORF A is required to promote ribosome shunt on the model mRNA leader. To determine the role of a uORF in shunting, its length, sequence, amino acid-encoding potential, and position should be further studied. We expect that an analysis of ribosome traffic on the artificial structured mRNA leader will allow easier evaluation of the shunt mechanism and kinetics of the shunting process.

MATERIALS AND METHODS

Thermodynamic calculations

Predictions of thermodynamically optimal secondary structures of RNA were performed using the Mfold program (37 °C, GCG Wisconsin Group package).

Chemicals and enzymes

All restriction endonucleases, SP6 RNA polymerase, Taq polymerase, Rapid DNA Ligation Kit, and CAT-ELISA assay were purchased from Boehringer; T4 DNA polymerase from New England Biolabs; RNase inhibitor, RQ1 RNase-free DNase, and the wheat germ extract from Promega; [S^{35}]-Met (1,000 Ci/mmol) and [α-P^{32}]-UTP (3,000 Ci/mmol) from Amersham.

Constructs and transcripts

CAT reporter gene expression under the influence of CaMV (strain S; Franck et al., 1980) 35S RNA leader (all numberings are according to Hemmings-Mieszczak et al., 1998) or artificial leader sequences was analyzed in vitro using pGEM-1-based constructs (Promega) or in transiently transfected *Orychophragmus violaceus* protoplasts using pDH51-based constructs (Pietrzak et al., 1986). Preparation of expression constructs and introduction of additional restriction sites (Fig. 2A; *Hin*dIII, *Xba*I, *Bam*HI, *Eco*RI, *Sal*I, *Spe*I, and *Nco*I) were described previously (Hemmings-Mieszczak et al., 1998). Mutations in the leader were introduced by pairs of annealed oligos subcloned between two relevant restriction sites. All constructs were sequenced; sequences of oligonucleotides and constructs are available on request.

SP6-directed transcripts were synthesized on templates digested with *Pst*I or *Eco*RI (constructs used in Figs. 4 and 6B did not contain *Eco*RI site in the leader) and used for in vitro translation assays giving the full-length or truncated CAT products, respectively. In the former case, the in vitro translated products were separated in the 12% sodium dodecyl sulfate–polyacrylamide gel electrophoresis (SDS-PAGE); in the latter case the separation was performed in the 16.5% SDS-PAGE using the Tricine discontinuous buffer system (Schägger & von Jagow, 1987).

Translation

Translation in cell-free system from wheat-germ and transient expression assays in protoplasts from *O. violaceus* were performed exactly as described previously (Hemmings-Mieszczak et al., 1998).

Immunoprecipitation assay

For immunodetection, the C-terminal uORF F extension into the CAT ORF (GEKNHWIYHR*; present on wt and pMH161,

pMH162, pMH163, pMH172, and pMH215 constructs) was replaced by the HA-epitope (MYPYDVPDYA*; present on the wt′, and pMH161′, pMH162′, pMH63′, pMH172′, and pMH215′ constructs). SP6-directed transcripts were synthesized on templates digested with *Pst*I and used for in vitro translation at 50 mM KOAc in 60 μL reactions: 10 μL were directly analyzed electrophoretically; the rest (50 μL) was immunoprecipitated with the anti-HA epitope 12CA5 monoclonal antibody coupled to protein A-Sepharose, as described by Andjelković et al. (1997). Products were separated in the 16.5% SDS-PAGE using the Tricine discontinuous buffer system (Schägger & von Jagow, 1987), the gel was fixed, dried, and exposed to the X-ray film (Kodak Biomax MR) for one week at −70 °C.

ACKNOWLEDGMENTS

We thank Matthias Müller and Dave Kirk for technical assistance and Drs. Margaret Collinge, Witold Filipowicz, and Helen Rothnie for commenting on the manuscript.

Received February 19, 1999; returned for revision March 19, 1999; revised manuscript received June 22, 1999

REFERENCES

Andjelković M, Alessi DR, Meier R, Fernandez A, Lamb NJC, Frech M, Cron P, Cohen P, Lucocq JM, Hemmings BA. 1997. Role of translocation in the activation and function of protein kinase B. *J Biol Chem 272*:31515–31524.

Belsham GJ. 1992. Dual initiation sites of protein synthesis on foot-and-mouth disease virus RNA are selected following internal entry and scanning of ribosomes in vivo. *EMBO J 11*:1106–1110.

Curran J, Kolakofsky D. 1988. Scanning independent ribosomal initiation of the sendai virus X protein. *EMBO J 7*:2869–2874.

Curran J, Kolakofsky D. 1989. Scanning independent ribosomal initiation of the sendai virus Y protein in vitro and in vivo. *EMBO J 8*:521–526.

Dominguez D, Ryabova LA, Pooggin MM, Schmidt-Puchta W, Fütterer J, Hohn T. 1998. Ribosome shunting in cauliflower mosaic virus. *J Biol Chem 273*:3669–3678.

Franck A, Guilley H, Jonard G, Richards K, Hirth L. 1980. Nucleotide sequence of cauliflower mosaic virus DNA. *Cell 21*:285–294.

Fütterer J, Gordon K, Pfeiffer P, Sanfaçon H, Pisan B, Bonneville J, Hohn T. 1989. Differential inhibition of downstream gene expression by the cauliflower mosaic virus 35S RNA leader. *Virus Genes 3*:45–55.

Fütterer J, Kiss-László Z, Hohn T. 1993. Nonlinear ribosome migration on cauliflower mosaic virus 35S RNA. *Cell 73*:789–802.

Fütterer J, Potrykus I, Bao Y, Li L, Burns TM, Hull R, Hohn T. 1996. Position-dependent ATT initiation during plant pararetrovirus rice tungro bacilliform virus translation. *J Virol 70*:2999–3010.

Geballe AP, Morris DR. 1994. Initiation codons within 5′-leaders of mRNA as regulators of translation. *Trends Biochem Sci 19*:159–164.

Gray NK, Hentze MW. 1994. Iron regulatory protein prevents binding of the 43S translation pre-initiation complex to ferritin and eALAS mRNA. *EMBO J 13*:3882–3891.

Hemmings-Mieszczak MW, Steger G, Hohn T. 1997. Alternative structures of the cauliflower mosaic virus 35S RNA leader: Implications for viral expression and replication. *J Mol Biol 267*:1075–1088.

Hemmings-Mieszczak MW, Steger G, Hohn T. 1998. Regulation of CaMV 35S RNA translation is mediated by a stable hairpin in the leader. *RNA 4*:101–111.

Hinnenbusch AG. 1994. Translational control of GCN4: An in vivo barometer of initiation-factory activity. *Trends Biochem Sci 19*:409–414.

Kaminski A, Howell MT, Jackson RJ. 1990. Initiation of encephalomyocarditis virus RNA translation: The authentic initiation site is not selected by a scanning mechanism. *EMBO J 9*:3753–3759.

Kozak M. 1986. Influences of mRNA secondary structure on initiation by eukaryotic ribosomes. *Proc Natl Acad Sci USA 83*:2850–2854.

Kozak M. 1989a. Circumstances and mechanism of inhibition of translation by secondary structure in eukaryotic mRNAs. *Mol Cell Biol 9*:5134–51142.

Kozak M. 1989b. The scanning model for translation: An update. *J Cell Biol 108*:229–241.

Kozak M. 1992. A consideration of alternative models for the initiation of translation in eukaryotes. *Crit Rev Biochem Mol Biol 27*:385–402.

Li J. 1996. Molecular analysis of late gene expression in budgerigar fledgling disease virus. Ph.D. thesis, University of Giessen, Giessen, Germany.

Pelletier J, Sonenberg N. 1985. Insertion mutagenesis to increase secondary structure with the 5′ noncoding region of a eukaryotic mRNA reduces translational efficiency. *Cell 40*:515–526.

Pelletier J, Sonenberg N. 1988. Internal initiation of translation of eukaryotic mRNA directed by a sequence derived from poliovirus RNA. *Nature 334*:320–325.

Pietrzak M, Shillito M, Hohn T, Potrykus I. 1986. Expression in plants of two bacterial antibiotic resistance genes after protoplast transformation with a new plant expression vector. *Nucleic Acids Res 14*:5857–5868.

Pilipenko EV, Gmyl AP, Maslova SV, Svitkin YV, Sinyakov AN, Agol VI. 1992. Prokaryotic-like *cis* elements in the cap-independent internal initiation of translation on picornavirus RNA. *Cell 68*:119–131.

Pooggin MM, Hohn T, Fütterer J. 1998. Forced evolution reveals the importance of short open reading frame A and secondary structure in the cauliflower mosaic virus 35S RNA leader. *J Virol 72*:4157–4169.

Schägger H, von Jagow G. 1987. Tricine-sodium dodecyl sulfate-polyacrylamide gel electrophoresis for the separation of proteins in the range from 1 to 100 kDa. *Anal Biochem 166*:368–379.

Schärer-Hernández N, Hohn T. 1998. Nonlinear ribosome migration on cauliflower mosaic virus 35S RNA in transgenic tobacco plants. *Virology 242*:403–413.

Scheper GC, Voorma HO, Thomas AAM. 1994. Base pairing with 18S ribosomal RNA in internal initiation of translation. *FEBS Lett 352*:271–275.

Schmidt-Puchta W, Dominguez D, Lewetag D, Hohn T. 1997. Plant ribosome shunting in vitro. *Nucleic Acids Res 25*:2854–2860.

Stripecke R, Oliveira CC, McCarthy JEC, Hentze MW. 1994. Proteins binding to 5′ untranslated region sites: A general mechanism for translational regulation of mRNAs in human and yeast cells. *Mol Cell Biol 14*:5988–5909.

Yueh A, Schneider RJ. 1996 Selective translation initiation by ribosome jumping in adenovirus-infected and heat-shocked cells. *Genes & Dev 10*:1557–1567.